Parametrisation Scheme for Multidisciplinary Design Analysis and Optimisation of a Floating Offshore Wind Turbine Substructure – OC3 5MW Case Study

Adebayo Ojo[1], Maurizio Collu[2], Andrea Coraddu[3]

[1,2]Department of Naval Architecture Ocean and Marine Engineering, University of Strathclyde, Glasgow G4 0LZ, UK;
[3]Department of Maritime & Transport Technology, Delft University of Technology, 2628 CD Delft, The Netherland.

adebayo.ojo@strath.ac.uk

Abstract. The development of novel energy technologies is considered imperative in the provision of solutions to meet an increasing global demand for clean energy. Floating Offshore Wind Turbine (FOWT) is one of the emerging technologies to exploit the vast wind resources available in deeper waters. To lower the levelized cost of energy (LCOE) or optimise the performance response associated with a FOWT system, a detailed understanding of the different disciplines (Aero-Hydro-Servo-Elastic) within the system and the relationship between the FOWT system and the dynamics of the marine environment is required. This requires an efficient Multidisciplinary Design, Analysis and Optimisation (MDAO) framework for FOWT systems to reduce the capital cost and increase dynamic performance. A key component of any MDAO framework is the shape parameterisation scheme, as it enables the modelling of a large array of platform designs with different geometric shapes using limited number of parameters. This work focuses on the B-Spline parameterisation modelling technique of OC3 spar-buoy and the use pattern search optimization algorithm to select the optimal design variants. The parametrisation technique is implemented in an analysis framework, where a B-spline library from Sesam GeniE is used to model each design representation, and a potential flow frequency domain analysis solver (HydroD/Wadam) is used for the hydrodynamic analysis. Validation of the selected designs within the design space is conducted with a benchmark NREL5MW spar-buoy hydrodynamic response results in literature with the hydrodynamic response of the frequency domain modelling approach using Sesam GeniE and HydroD/Wadam. This analysis process shows a high accuracy in response results between the OC3 spar-buoy in literature and the OC3 spar-buoy model design using B-Spline parametrization technique. Key performance metrics like the cost of materials and root mean square (RMS) of the nacelle acceleration also show improvement with the design variants compared to estimation from OC3 design in literature.
Keywords: Frequency domain, optimisation algorithm, parameterization, B-spline, MDAO.

1. Introduction

The reduction of greenhouse gases across the entire globe requires adequate implementation of different renewable energy technologies, amongst which is the technology of floating offshore wind turbine (FOWT). The FOWT concept dates back to 1972, when it was initially proposed by Heronemus [1]. It is a multidisciplinary engineering system that is capable of exploiting/harnessing the vast wind resources available and reducing the substantial capital cost outlays that could be expended on fixed bottom

foundation if adapted for deep waters. To make this technology attractive, though, requires lowering the levelized cost of energy (LCOE).

Three main floating platform concepts (spar, semisubmersible, and tension leg platform) from the oil and gas industry are being adopted as the early to market floaters in the offshore wind industry. In the offshore wind, the parameterization scheme adopted for the floating substructures are mainly centered around varying the diameters and the draft of the platforms as detailed in the work of Tracy [2] and Sclavounos et al [3]. In [2], the results of the parametric study show a number of designs that highlights Pareto fronts for mean square acceleration of the turbine versus multiple cost drivers (displacement of floaters and mooring line tension) for the offshore structure. The work from Sclavounos et al [3] shows that when a fully coupled dynamic analysis conducted for the FOWT system including the turbine, floater and the mooring system under both wind and sea state environmental conditions, the Pareto optimal structures are generally either a narrow deep drafted spar or a shallow barge ballasted with concrete. The parametrization technique in [2] and [3] limits the design space as the varying parameters are the diameter and the draft. Access to a richer design space can be achieved by altering the shapes of the floaters.

Unlocking the optimal design shapes of the floaters within the multidisciplinary framework requires the understanding of different shape parametric designs techniques used in other multidisciplinary environments like aerospace and automotive industries. These state-of-the-art parameterization techniques have been reviewed in the work of Samareh et al [4] and they are: basis vector technique, domain element technique, partial differential equation technique, discrete technique, CAD geometry technique, free form deformation (FFD) technique, and polynomial spline, from which the B-Spline technique is derived. The parameterization technique adapted in this work is the polynomial spline. Polynomial and splines have been vastly used in engineering design from the aerospace and automobile sectors to the naval architecture sectors as most CAD modellings are based on splines [5]. The number of variables needed to generate a smooth shape can be greatly reduced by using a spline representation [5]. In the work of de Menezes et al. [6], the B-Spline panel model is input to the wave analysis MIT (WAMIT) system in the required format for the frequency domain analysis of hull motion response to waves. The quality of the results obtained with B-Splines modelling was compared to the ones obtained with flat panels. B-Splines have shown to be an effective approach, more efficient in computing terms when compared with the flat panels approach and suitable to optimization scripts [6]. It revealed itself as a more adequate procedure to the design work as it simplifies the hull form mathematical definition of floating systems [6]. In the work of Liu et al [7], which highlights the development of a semi-submersible floating offshore platform with a catenary mooring system to support a very large 13.2-MW wind turbine with 100-m blades, the hydrodynamic assessment of the platform was conducted using WAMIT. The accuracy of the WAMIT result was improved using a B-Spline surface modelling which provides a high-order representation of all geometric descriptions required in the finite element mesh used by WAMIT. This work shows that the application of potential flow theory to the platform model is justified as computed hydrodynamic coefficients for the model are consistent with the OC4 DeepCwind model [7]. Design and optimization approaches for offshore wind turbines can be divided into various methods amongst which are optimization based on static analysis approach, frequency domain approach and time domain approach [8]. The optimizers can be derivative based or meta-heuristic-based optimizers. Optimization based on frequency domain analysis has the advantage of lower computational cost over optimization based on the time-domain analysis [8]. A review of optimization based on frequency domain analysis is detailed in the work of Gentils et al [9] in which they minimized the mass of the support structure under multi criteria constraints for a 5MW offshore wind turbine for an OC3 monopile using a Genetic Algorithm (GA). Some optimization constraints used in this study are buckling, stress, vibration and fatigue. The optimal result shows a 20% reduction in the global mass of the support structure design is achievable [9]. Further work on the optimization of an offshore platform based on the frequency domain approach was conducted by Hall et al [10] and subsequently fine-tuned by Karimi et al [11]. Hall et al [10], conducted a study on the hull shape and mooring line optimization of FOWT across different platform categories using a GA and a frequency

domain approach with a linear representation of the hydrodynamic viscous damping. The GA is applied for single and multi-objective optimization, and the results indicate an un-conventional design that shows the necessity for cost function refinement. This work was improved by Karimi et al [11] using a Kriging-Bat optimization algorithm (a surrogate-based meta-heuristic optimization algorithm) and a linearized frequency domain dynamic model. Unlike [10], this showed improved correlation between cost and substructure design.

The optimization for the parameterization design models of this work is based on the frequency domain analysis using the panel method to solve a potential flow problem and selection of the optimal design is based on the meta-heuristic pattern search optimization algorithm[12]. The tools used are MATLAB for optimization, Sesam Genie with B-Spline library with control point shape alteration feature for panel modelling, and finite element mesh generation of the OC3 spar-buoy base model and other design variants and HydroD/Wadam to investigate system's responses in the frequency domain.

The work conducted in this paper is arranged as follows: Section 1 provides an introductory overview to the topic with a brief review of related work from literature, Section 2 gives an overview of the objectives and methodology, Section 3 looks at the use of the methodology on a standard NREL 5MW OC3 spar-buoy and compares the results with literature results, Section 4 uses the developed methodology to model and analyze the selected optimal variants from the OC3 spar-buoy while Section 5 discusses the results. Finally, Section 6 presents the main conclusions and recommendations.

2. Objectives and Methodology

Optimal design and analysis of a complex multidisciplinary system like a FOWT is an iterative process [13] that can be computationally expensive. Presently, most wind turbines are rated based on their power output [14] and each rated turbine comes with a specific design of the rotor nacelle assembly. To complete this system is the substructure platform and, in some cases, tower that has to be designed and coupled with the rest of the multidisciplinary system including the rotor nacelle assembly (RNA) to optimally satisfy the design requirements. For an efficient development of offshore platforms and to avoid the iterative process to identify an optimal design, an efficient parametric process integrated with design and analysis optimization is essential. The main objective of this work is the definition of a robust, efficient shape parameterization approach for floating wind turbine support structures and the exploration of the design space with an optimization algorithm. This involves representing the model's shape with very few finite numbers of variables to minimize computation cost and integrating it with an optimizer to identify an optimal solution of the design model. Parametric modelling capabilities lead to the generation of innovative geometries and subsequent optimization for platform designs. Only shapes that can be feasibly modelled and provide possible solutions to the optimization problem [13] are selected. The proposed methodology for the parametric analysis of a FOWT substructure is to firstly define a parameterization scheme with a robust design space configuration using the B-spline parameterization technique. The next stage is to conduct analyses of design models within the design space with frequency domain analysis tools like the Sesam suite by DNV (Genie and HydroD/Wadam). The penultimate stage is to integrate the analysis with the optimizer for optimal design selection. Finally, the design is validated by comparing a benchmark OC3 spar-buoy model response results with the OC3 spar-buoy results in literature. This methodological process is highlighted in Figure 1.

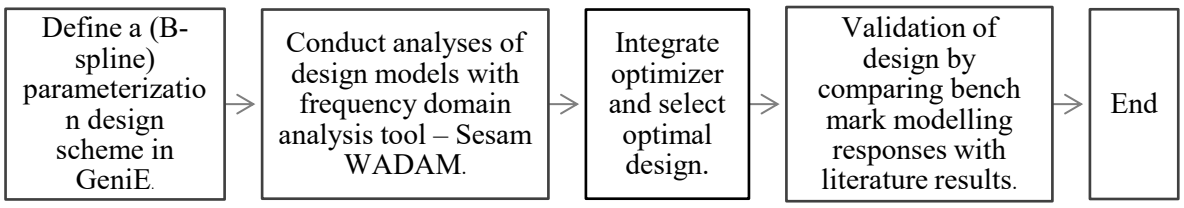

Figure 1. Parametric optimisation process for a floating platform

3. OC3 Phase IV Spar-Buoy FOWT (B-Spline model and frequency domain analysis)

The OC3 phase IV spar-buoy floater is based on the Hywind spar-buoy and modified to support the NREL 5MW reference wind turbine [15]. Comparison of the structural parameter values shows that the dimensions, apart from the improved and reduced draft of the real systems, lie between the dimensions of the Hywind Demo for a 2.3MW wind turbine and the Hywind Scotland floater supporting a 6.0 MW wind turbine [16]. A representative model sketch of the OC3 spar-buoy is shown in Figure 2. Details of the geometric and structural parameters like the mass of the spar-buoy and ballast, center of mass, degree of freedom inertias and additional linear damping in surge, sway and yaw are presented in [15], [16] and [17]. For the purpose of this study, the tools used for the design and analysis of the phase IV OC3 spar-buoy is the Sesam suite (GeniE and Wadam) by DNV [18]. GeniE is a tool for concept / high level modelling of beams, stiffened plates, shells and curved edges, used to create the finite element mesh (FEM) file (representing the design characteristic of the floating wind turbine support structure) to HydroD/Wadam for hydrostatic stability and hydrodynamic analysis, to determine the response motion of the system. GeniE has an extensive library of guiding geometry tools that helps create beams, plates and curved surfaces. Some of these tools are circular / elliptic arcs, cubic splines, B-splines, polycurves and polynomials.

B-spline curve from GeniE is used to model the spar-buoy substructure with 12 control points representing the radii along with the draft of the platform, as presented in Table 1. The model from the data in Table 1 is highlighted in Figure 3. The thickness of the platform is estimated using Excel's scenario analysis. The steel mass of the spar-buoy platform is 0.13 of the buoyancy mass of the spar-buoy platform [19]. The formula for the steel mass of the platform incorporating the spar-buoy thickness as an unknown is set to be equals to the value of 0.13 of the buoyancy mass of spar as specified in [19]. With this, the scenario analysis derives the accurate thickness value that corresponds the target value of the steel mass' fraction of the buoyancy mass. For this setting, that target value search results is a wall thickness of 0.0418m along the entire length of the spar-buoy.

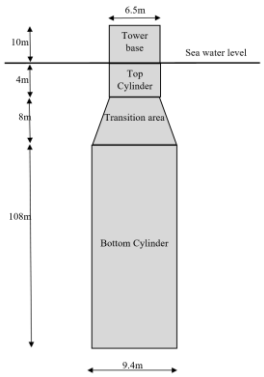

Figure 2. OC3 Spar-buoy Sketch

Figure 3. B-spline model of an OC3 FOWT System with Sesam GeniE

Table 1. OC3 Spar-Buoy B-spline Curve

Height (m)	0	4	12	30	40	50	60	70	80	90	100	110	120
Radius (m)	3.25	3.25	4.7	4.7	4.7	4.7	4.7	4.7	4.7	4.7	4.7	4.7	4.7

The tower and RNA are modelled in GeniE as a dummy beam with the center of mass assigned to the dummy beam corresponding to the calculated center of mass of the tower and RNA. The dummy beam with the assigned center of mass is connected to the OC3 spar-buoy and meshed in GeniE. The FEM

model is taken to the Wadam solver for hydrodynamic analysis to investigate the system's response. Wadam uses the Morison equation [18] and first and second order 3D potential theory [18] for the wave load calculations in which the incident wave is an Airy wave and the analysis is performed in the frequency domain. The resultant system of equations of motion, in the frequency domain, for a FOWT body in regular waves is highlighted in equation (1), [20]-[21].

$$\sum_{j=1}^{6} \xi_j \left[-w^2\left(M_{kj} + a_{kj}\right) + iwb_{kj} + c_{kj}\right] = \eta X_k \qquad (1)$$
$$k = 1, \ldots, 6$$

Where M_{kj} is the total system mass matrix, a_{kj} is the hydrodynamic added mass coefficient, b_{kj} is the radiation damping coefficient without the consideration of viscous forces, and c_{kj} is the sum of the hydrostatic and mooring stiffness coefficients. ξ_j is the j-th degrees of freedom displacement (rigid platform global response), η is the wave amplitude and X_k is the first order wave load transfer function [20]-[21]. The complex response transfer function between the amplitude of the wave and the amplitude of oscillation in the oscillatory degrees of freedom is highlighted in equation (2).

$$H_j = \frac{\xi_j}{\eta} = \sum_{k=1}^{6} \frac{X_k}{-w^2\left(M_{kj} + a_{kj}\right) + iwb_{kj} + c_{kj}} \qquad (2)$$

The response amplitude operator (RAO) in the j^{th} degree of freedom is defined as the complex magnitude of the transfer function H_j as highlighted in equation (3) .

$$RAO_j = \left|H_j\right| \qquad (3)$$

3.1. Results and System Responses for OC3 spar-buoy

Using the B-spline parametric modelling technique from Sesame GeniE to model the OC3 spar-buoy with data from Table 1, and conducting hydrodynamic analysis using the panel model option in Wadam / HydroD, a host of results are extracted and compared with literature results as highlighted in this section. The results demonstrate there is an agreement/alignment between the modelling framework (B-spline modelling technique in GeniE coupled with the hydrodynamic analysis in HydroD/Wadam) results and the results of the OC3 hydrodynamic analysis available in literature. Figure 4 shows that the linear and rotational degrees of freedom added mass coefficients for the analysed B-spline model match the model from literature [15] using OpenFAST in magnitude and trend. The same observation is replicated in Figure 5, which represents the damping coefficient (linear and rotational DOF). The surge, heave, and pitch excitation forces and moments are also aligned between the model analyzed and literature values [15] as shown in Figure 6.

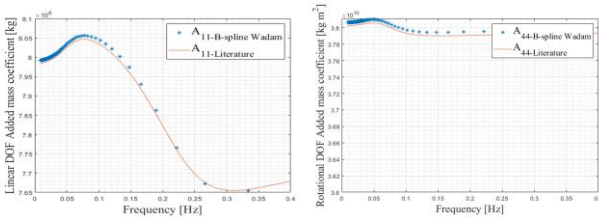

Figure 4. Added mass coefficients (B-spline model vs literature model)

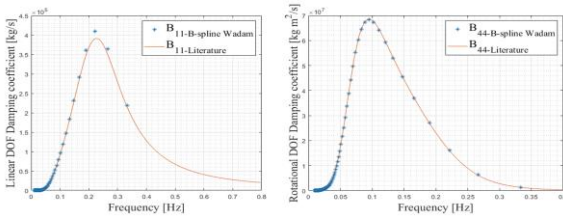

Figure 5. Damping coefficients (B-spline model vs literature model)

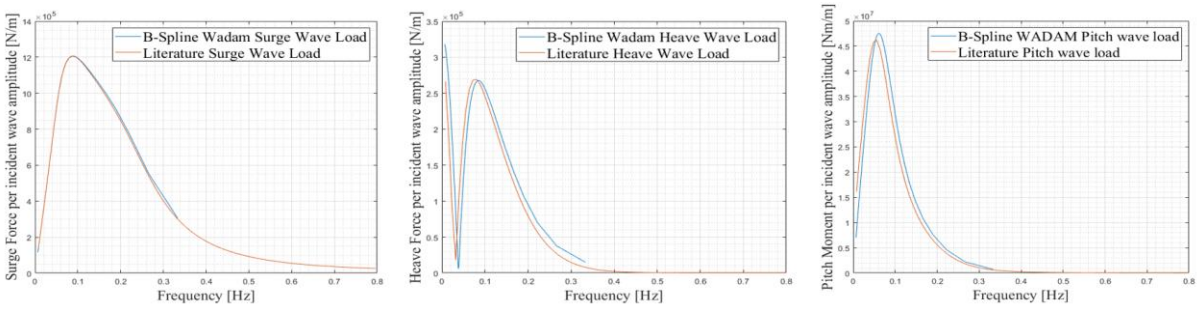

Figure 6. Excitation loads and moment (B-spline model vs literature model)

The system's response amplitude operator in surge, heave and pitch DOF's are compared between B-spline model and literature values [14] in Figure 7. The comparison shows agreement between the B-spline modelling methodology with GeniE modelling and Wadam analysis and the plot from literature conducted by Ramachandran et al. [14]. With a high level of accuracy established between the RAO's of a frequency domain analytical procedure using B-Spline parametric design and potential theory for hydrodynamic analysis, larger and richer design space can be explored with optimisation algorithm for this high-level analysis in frequency domain to select optimal design as detailed in Section 4.

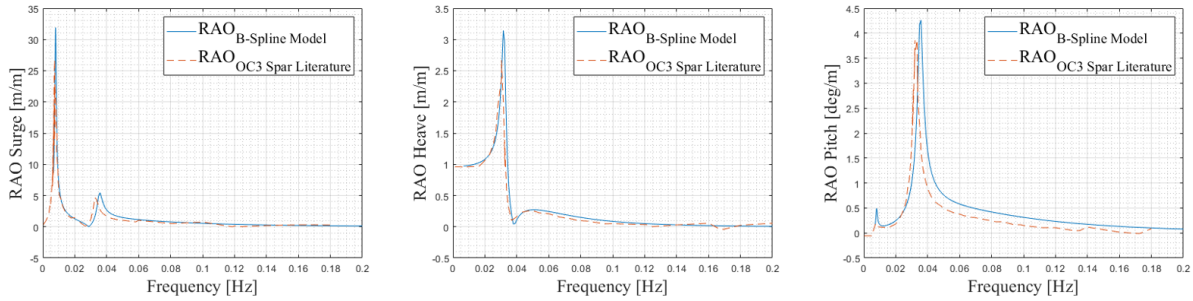

Figure 7. Surge, Heave and Pitch RAO (B-spline model vs literature model)

4. Optimal Designs and Parametric Model of Selected Design Variants from NREL 5MW OC3 Spar FOWT

B-Spline parametric modelling technique is used to model the OC3 Spar FOWT. The optimisation framework is conducted with the control points of the B-Spline curve used as the design variable in the optimization scheme. This allows for shape variation and optimisation of the design model to satisfy the requirements of stability, cost minimisation and acceptable hydrodynamic performance. The formulation of a general design optimisation is defined in the context of minimising or in some cases maximising an objective function subject to constraints. This statement, in the context of minimizing objective function can be represented as expressed in equations (4) to (8).

Find:

$$\hat{x} = [x_1, x_2, \ldots, x_k] \quad (4)$$

That minimizes

$$\hat{f}(x) \quad (5)$$

Subject to

$$\hat{x}lower \leq \hat{x} \leq \hat{x}upper \quad (6)$$

$$h_i(x) = 0; i = 1\ to\ m \quad (7)$$

$$g_j(x) \leq 0; j = 1\ to\ p \quad (8)$$

Where $\hat{f}(x)$ is an objective function minimized with respect to the design variables $\hat{x}$, m is the number of equality constraints, and p is the number of inequality constraints.

The FEDORA multidisciplinary analysis (MDA) in-house framework developed by researchers in Strathclyde University using a simpler parameterization scheme to discover unique configurations with reduced structural mass that can lead to cost savings. The FEDORA MDA was integrated with the pattern search optimization algorithm tool in MATLAB [22] for the optimal selection of designs describing rougher shapes. This work improves the FEDORA MDA by using the DNV Sesam suite GeniE and WADAM with the B-Spline parameterization feature in Sesam GeniE capable of using a few design variables to describe more advanced unique shape than FEDORA MDA. The flexibility of the B-Spline curve in GeniE to change the specific segment of the curve around the control point when the control point variables are changed enables the realization of richer designs.

The B-Spline control points' data to model the selected design is presented in Table 2. In Table 2, the B-Spline curve for each design has 12 control points along the vertical axis and is swept round the radii at the control points to create the platform. The single objective function of the optimization study is the cost of the steel material utilized for the floating substructure, with the ballast cost considered negligible. Four constraints are considered as highlighted below, with the first three constraints kept as constant while the fourth constraint varies. The constraints are:

1. A ballast mass greater than zero, ensuring floatability
2. A nacelle acceleration less than the maximum allowable operational acceleration of the nacelle
3. A positive roll/pitch initial stiffness (mathematically, constraint no.4 can be satisfied with a negative initial stiffness), to avoid non-physical solutions.
4. The maximum pitch angle of inclination (the sum of the static and dynamic pitch angles) does not exceed the total operational maximum pitch angle of inclination.

The maximum pitch angle of inclination (static and dynamic) is varied, defining four cases: 10 degrees, 7.5 degrees, 5 degrees and 7 degrees. The control points and radii at each control point along the vertical axis of the four optimal parametric designs and their geometries are highlighted in Table 2 and Figure 8 respectively as cases A, B, C and D for maximum pitch angles of 10 degrees, 7.5 degrees, 5 degrees and 7 degrees respectively. All the cases are coupled with the NREL 5MW wind turbine and tower, exposed to the same sea state and the system's responses are calculated.

Table 2. Design data for selected models

Case A (m)	Height	0	10	20	30	40	50	60	70	80	90	100	110	120
	Radius	3.72	4.13	4.01	3.89	3.77	3.65	3.54	2.64	0.50	0.50	0.50	3.65	3.71
Case B (m)	Height	0	10	20	30	40	50	60	70	80	90	100	110	120
	Radius	4.03	4.72	4.52	4.29	4.08	3.88	3.69	0.98	0.50	0.50	0.50	3.95	4.06
Case C (m)	Height	0	10	20	30	40	50	60	70	80	90	100	110	120
	Radius	6.91	6.86	7.22	6.04	5.00	0.55	0.50	0.50	0.50	0.50	0.53	3.38	3.92
Case D (m)	Height	0	10	20	30	40	50	60	70	80	90	100	110	120
	Radius	4.13	4.92	4.69	4.42	4.18	3.95	3.48	0.72	0.50	0.50	0.50	4.05	4.18

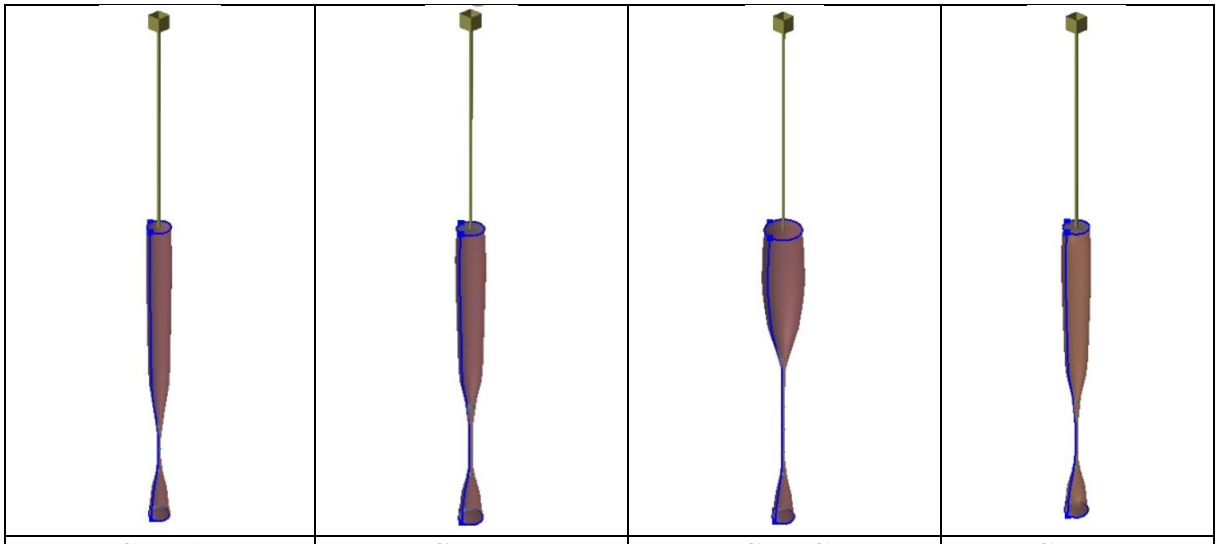

Case A	Case B	Case C	Case D

Figure 8: Selected models from pattern search optimization algorithm

The model for each case is produced with B-Spline curve and a material density of 7850kg/m3 (Steel) is applied. A wall thickness of 0.0418m derived from the use of the ratio of steel mass to buoyancy mass of 0.13 [19], [23] was applied using the buoyancy mass of the NREL OC3 platform as a target value to select the wall thickness. On completion of the model, the Sesam Genie is used to generate the finite element mesh (FEM) files. The hydrodynamics analyses for the four cases are conducted with the Wave Analysis by Diffraction and Morison theory (Wadam) tool in the HydroD software within the DNV Sesam suite. The total mass of the system (wind turbine, support platform and ballast) and the center of gravity of the system is determined in Wadam. Figure 8 shows the optimal spar generated for the four cases are geometrically different from the conventional Spar in Figure 3. It is anticipated that any manufacturing issues can be addressed with additive manufacturing or other techniques like the slip forming of concrete spar.

4.1. Wave Spectrum

The analyses of offshore wind turbines can be conducted with different design load cases as highlighted in various recommended standards [24] to [29]. For the purpose of this study, the wave spectrum of interest is the JONSWAP wave spectrum and environmental parameters are provided in Table 3.

Table 3. Environmental data for wave spectrum

Wave parameters		
Hs (meters)	10.37	Significant wave height of the spectrum
Tp (seconds)	14.70	Peak period of the wave spectrum
Peak /Gamma factor	3.30	Non-dimensional peak shape parameter
σ_1	0.07	Spectral width parameter for angular frequency <= peak angular frequency
σ_2	0.09	Spectral width parameter for angular frequency > peak angular frequency

The JONSWAP wave spectrum is represented with the expression in equation (9) as detailed in [30]

$$s(f) = \frac{\alpha g^2}{16\pi^4} f^{-5} exp\left[-\frac{5}{4}\left(\frac{f}{f_m}\right)^{-4}\right]\gamma^b \qquad (9)$$

$$\mathrm{b} = \exp\left[-\frac{1}{2\sigma^2}\left(\frac{f}{f_m}-1\right)^2\right]$$

$$\sigma = \begin{cases} \sigma_1 & for\ f \leq f_m \\ \sigma_2 & for\ f > f_m \end{cases}$$

Where α is the Philips constant, γ is the peakedness parameter, f is the frequency in Hertz, f_m is the peak frequency in Hertz, g is the acceleration due to gravity in m/s^2 and *s(f)* is the energy spectrum from the waves in m^{2}s. Applying the parameters in Table 3 into equation (9), the peak power for the wave spectrum is 305 m^2/Hz at 14.7 Seconds (peak period).

5. Results of Selected Design Variants from NREL 5MW OC3 Spar-buoy FOWT

This section highlights the system's response which are intrinsic design characteristics of the model. The system's responses are determined for all the four cases and plotted in comparison to the OC3 NREL 5MW FOWT system. Figure 9 shows the RAOs in surge, heave, pitch, and horizontal nacelle displacement motion for the four design variant cases and the OC3 spar-buoy. It is shown in Figure 9 that case A design has the largest peak motion response in surge, pitch and the nacelle horizontal displacement with values of about 45m/m, 15deg/m and 68m/m respectively while case C has the largest peak motion response in heave of about 6.8m/m. This analysis did not consider any viscous forces and lower peaks are expected if viscous forces are taken into account. From an operational perspective, case A will exhibit largest motion in all considered DOF apart from the heave DOF where case C shows the largest motion. Further details of the material estimates are highlighted in the performance metric section. Also, the frequency of occurrence of the peak response motions in surge pitch and nacelle displacement is between 0 and 0.04Hz while it is between 0.02Hz and 0.08Hz for heave motion.

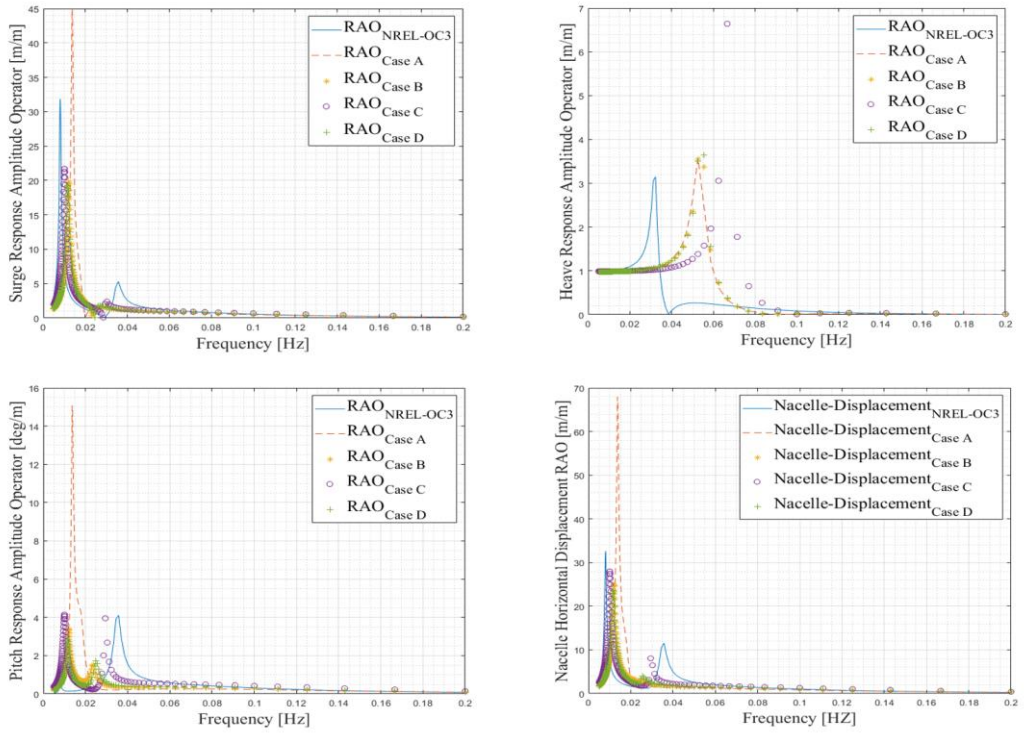

Figure 9.Surge, Heave, Pitch and Nacelle displacement RAO for all three cases and the OC3 spar

The system's response in surge, heave, pitch, nacelle displacement and nacelle acceleration to the wave spectrum considered can be estimated with the sea-state provided in Table 3. From the highlighted responses, the nacelle acceleration RMS can be estimated from equation (10) and values for each case presented in Table 5.

$$m_0 = \int_{f=0}^{f=+\infty} S_{Nac\_accl}(f)\mathrm{d}f \quad (10)$$

Where *S(Nac_accl)* is the nacelle acceleration response spectrum and f is frequency of the sea state wave spectrum.

5.1. Performance Metrics

Key performance metrics or fitness functions are applied to evaluate the selected designs. The performance metrics for evaluation of selected designs are the platform's mass as an approximate measure of the cost of steel or concrete and the nacelle acceleration RMS.

5.1.1. Platform Mass: The platform mass for all selected cases and the corresponding cost based on steel and concrete is highlighted in Table 4. Comparison of the masses between the selected design is shown in Figure 10, while the corresponding cost between the steel and concrete is compared for each selected design case in Figure 11. The cost of steel and concrete used for the total cost estimation are 537GBP/tonne and 77GBP/tonne as specified in Ioannou et al. [31]. The results in Table 4 shows that the OC3 spar-buoy has the biggest mass and most expensive in terms of cost. It should be noted that the estimation of the masses in Table 4 is approximated. For a detailed design, other constraints like the structural integrity and safety factors for operational use of the system would be taken into consideration and that would likely lead to a mass value close to the OC3 platform.

Table 4. Platform mass and corresponding cost estimate

Platform Type	Mass (Tonnes)	Cost- Steel (GBP)	Cost-Concrete (GBP)
OC3	1069.86	575E+03	824E+02
Case A	736.55	396E+03	567E+02
Case B	771.84	414E+03	594E+02
Case C	811.29	436E+03	625E+02
Case D	781.84	420E+03	602E+02

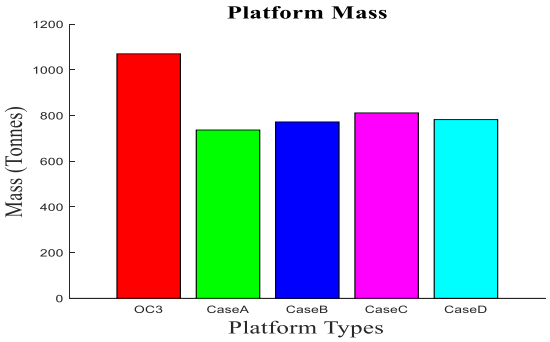

Figure 10. Mass of selected platforms

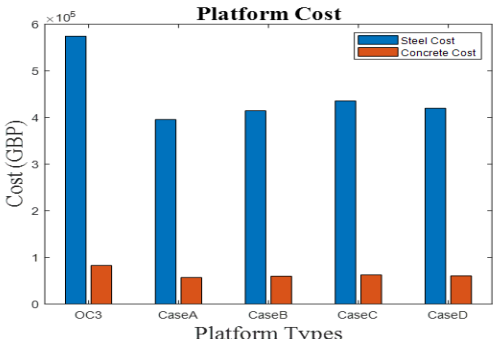

Figure 11. Cost of selected platform designs from steel and concrete materials

5.1.2. Nacelle Acceleration RMS: An important key performance metric for the selected designs is the nacelle acceleration RMS value. Common operational limit for the maximum allowable nacelle acceleration is between 20% and 30% of the gravitational acceleration (g) [32], [33] which corresponds to an acceleration of about 1.962 m/s^2 to 2.943 m/s^2 The values of the nacelle acceleration RMS for the designs selected are presented in Table 5 and it shows that case C has the highest value of 0.0816m/s^2

which is larger than the benchmark nacelle acceleration recorded for the NREL 5MW OC3 spar-buoy at 0.0777m/s^2. Case D is a variant from the OC3 spar-buoy with a maximum pitch angle that is the same as that used in the OC3 design and it can be seen that the case D design exhibits a much-improved nacelle acceleration RMS than the standard OC3 spar-buoy. This shows that with the same constraint, pattern search optimisation with B-spline modelling could lead to a more accurate estimation of optimal design variant from a parent design.

Table 5. Nacelle acceleration RMS across selected designs

	OC3 Spar	**Case A**	**Case B**	**Case C**	**Case D**
Zeroth Moment (m/s^2)	0.0060	0.0029	0.0038	0.0067	0.0042
Nacelle Acceleration RMS(m/s^2)	0.0777	0.0534	0.0617	0.0816	0.0645

6. Conclusions and Recommendations

The purpose of this work is to highlight the use of the B-spline parametric modelling technique and pattern search optimisation algorithm for modelling and selecting optimal design variants from a benchmark NREL OC3 spar-buoy platform. Using the pattern search optimisation frame work, with cost of steel material as objective function and four sets of constraints highlighted in this paper, four optimal design variants of Case A, B, C and D are respectively selected from the OC3 spar-buoy.

The designs are modelled using B-Spline library from Sesame GeniE, and analysed with frequency domain hydrodynamic analysis approach using the Panel method in Sesam HydroD/Wadam. Key performance metrics (Cost and Nacelle acceleration RMS) were used to evaluate the analyses and benchmark them against the OC3. It can be concluded that the four optimized variants utilized less material than the OC3; hence lower cost of materials with case A using the least of the materials. However, quantity of material for the optimal design can be close to the OC3 platform when other constraints like the structural integrity, safety factors for operational use of the system are taken into consideration. Also, all the calculated nacelle accelerations for the four optimal designs are within the recommended operational limit for the maximum allowable nacelle acceleration (20% and 30% of (g)). This work shows that B-spline parametric design and optimization framework can be used to generate new concept designs or validate the selection of optimal designs while saving computational time and costs.

References

[1] Heronemus WE, Marine Technology S. Pollution-free energy from the offshore winds. [Washington, D.C.]: Marine Technology Society; 1972.
[2] Tracy CH. Parametric design of floating wind turbines: Massachusetts Institute of Technology; 2007.
[3] Sclavounos P, Tracy C, Lee S, editors. Floating offshore wind turbines: Responses in a seastate pareto optimal designs and economic assessment. International Conference on Offshore Mechanics and Arctic Engineering; 2008.
[4] Samareh JA, editor A survey of shape parameterization techniques. NASA Conference Publication; 1999: Citeseer.
[5] Samareh JA. Survey of shape parameterization techniques for high-fidelity multidisciplinary shape optimization. 2001;39(5):877-84.
[6] de Menezes FbGT, Dutra Martins Ps, editors. B-Splines Geometric Modeling for Dynamic Analysis Behaviour in Offshore Systems. 25th International Conference on Offshore Mechanics and Arctic Engineering; 2006.
[7] Liu J, Thomas E, Manuel L, Griffith DT, Ruehl KM, Barone MJJoMS, et al. Integrated system design for a large wind turbine supported on a moored semi-submersible platform. 2018;6(1):9.
[8] Chen J, Kim M-HJJoMS, Engineering. Review of Recent Offshore Wind Turbine Research and

Optimization Methodologies in Their Design. 2021;10(1):28.
[9] Gentils T, Wang L, Kolios AJAe. Integrated structural optimisation of offshore wind turbine support structures based on finite element analysis and genetic algorithm. 2017;199:187-204.
[10] Hall M, Buckham B, Crawford C, editors. Evolving offshore wind: A genetic algorithm-based support structure optimization framework for floating wind turbines. OCEANS 2013 MTS/IEEE Bergen: The Challenges of the Northern Dimension; 2013.
[11] Karimi M, Hall M, Buckham B, Crawford C. A multi-objective design optimization approach for floating offshore wind turbine support structures. Journal of Ocean Engineering and Marine Energy. 2017;3(1):69-87.
[12] Torczon V, Trosset MW, editors. From evolutionary operation to parallel direct search: Pattern search algorithms for numerical optimization. Computing Science and Statistics; 1998: Citeseer.
[13] Birk L, Clauss G, editors. Parametric hull design and automated optimization of offshore structures. 10th Int Congress of the Int Maritime Association of the Mediterranean, Hellas, Greece; 2002.
[14] Ramachandran G, Robertson A, Jonkman J, Masciola MD, editors. Investigation of response amplitude operators for floating offshore wind turbines. The Twenty-third International Offshore and Polar Engineering Conference; 2013: OnePetro.
[15] Jonkman J, Butterfield S, Musial W, Scott G. Definition of a 5-MW reference wind turbine for offshore system development. National Renewable Energy Lab.(NREL), Golden, CO (United States); 2009.
[16] Leimeister M, Kolios A, Collu M. Development and Verification of an Aero-Hydro-Servo-Elastic Coupled Model of Dynamics for FOWT, Based on the MoWiT Library. 2020;13(8):1974.
[17] Jonkman JM, editor Definition of the Floating System for Phase IV of OC32010.
[18] DNV. Sesam Feature Description. Software suite for hydrodynamic and structural analysis of renewable, offshore and maritime structures: DNV; 2021 [Available from: https://www.dnv.com/Images/Sesam-Feature-Description_tcm8-58834.pdf.
[19] Anaya-Lara O, Tande JO, Uhlen K, Merz K. Offshore Wind Energy Technology: John Wiley & Sons; 2018.
[20] Coraddu A, Oneto L, Kalikatzarakis M, Ilardi D, Collu M, editors. Floating Spar-Type Offshore Wind Turbine Hydrodynamic Response Characterisation: a Computational Cost Aware Approach. Global Oceans 2020: Singapore – US Gulf Coast; 2020 5-30 Oct. 2020.
[21] Newman JN. Marine hydrodynamics: The MIT press; 2018.
[22] MathWorks. MATLAB Global Optimization Toolbox - Pattern Search 2021 [Available from: https://uk.mathworks.com/help/gads/patternsearch.html.
[23] Collu M, Borg M. Design of floating offshore wind turbines. Offshore wind farms: Elsevier; 2016. p. 359-85.
[24] AS DG. Loads and Site Conditions for Wind Turbines: Standard DNVGL-ST-0437,. 2016.
[25] DNV. Design of Floating Wind Turbine Structures. 2013.
[26] DNVGL-ST-0119. Floating Wind Turbine Structures. 2018.
[27] IEC-61400-1. Wind Turbines—Part 1: Design Requirements, 3.1 ed., . 2014.
[28] IEC-61400-3-2. Wind energy generation systems – Part 3-2: Design Requirements for Floating Offshore Wind Turbines. . 2019.
[29] IEC-61400-3. Wind Turbines—Part 3: Design Requirements for Offshore Wind Turbines, 1.0 ed., . 2009.
[30] DNVGL Oslo, Norway. Class Guideline DNVGL CG 0130: Wave Loads. 2018.
[31] Ioannou A, Liang Y, Jalón ML, Brennan FP. A preliminary parametric techno-economic study of offshore wind floater concepts. Ocean Engineering. 2020;197:106937.
[32] Ch N, Ran L. Offshore Wind Farms: Technologies, Design and Operation2016. 1-634 p.
[33] Leimeister M, Kolios A, Collu M, Thomas P. Design optimization of the OC3 phase IV floating spar-buoy, based on global limit states. Ocean Engineering. 2020;202:107186.